Inimer Graft-Copolymerized Poly(vinylidene fluoride) for the Preparation of Arborescent Copolymers and "Surface-Active" Copolymer Membranes

ARTICLE *in* MACROMOLECULES · AUGUST 2004

Impact Factor: 5.8 · DOI: 10.1021/ma048894l

3 AUTHORS, INCLUDING:

Guangqun Zhai
Changzhou University
41 PUBLICATIONS **453** CITATIONS

SEE PROFILE

Inimer Graft-Copolymerized Poly(vinylidene fluoride) for the Preparation of Arborescent Copolymers and "Surface-Active" Copolymer Membranes

Guangqun Zhai, E. T. Kang,* and K. G. Neoh

Department of Chemical and Biomolecular Engineering, National University of Singapore, Kent Ridge, Singapore 119260

Received June 4, 2004; Revised Manuscript Received July 5, 2004

ABSTRACT: A novel graft copolymer was synthesized via graft copolymerization of an inimer, 2-(2-bromoisobutyryloxy)ethyl acrylate (BIEA), with ozone-pretreated poly(vinylidene fluoride) (PVDF) (the PVDF-*g*-PBIEA copolymer). Porous membranes could be fabricated from the copolymer solution by phase inversion. The BIEA polymer (PBIEA) side chains allowed the initiation of atom transfer radical polymerization (ATRP) of functional monomers on the copolymer and the membrane surface. An arborescent copolymer was prepared via ATRP of sodium 4-styrenesulfonate (NaSS) initiated from the PVDF-*g*-PBIEA copolymer side chains (PVDF-*g*-PBIEA-*ar*-NaPSS copolymer). In comparison with the PVDF-*g*-PBIEA-*ar*-NaPSS copolymer membrane cast in water by phase inversion, the copolymer membrane cast in 1 M aqueous NaCl solution had enriched NaPSS side chains on the surface and larger pore size. The PVDF-*g*-PBIEA-*ar*-PPEGMA membrane was prepared via the surface-initiated ATRP of poly(ethylene glycol) methacrylate (PEGMA) on the porous PVDF-*g*-PBIEA membrane. Protein adsorption studies indicated that the PVDF-*g*-PBIEA-*ar*-PPEGMA membrane exhibited substantially improved antifouling properties. Thus, the PVDF-*g*-PBIEA membranes with the active ATRP inimer repeat units on the surface offers opportunities for the functionalization of membranes via surface molecular design.

1. Introduction

Poly(vinylidene fluoride) (PVDF) has attracted considerable attention in recent decades because it is capable of exhibiting ferroelectric, piezoelectric, and pyroelectric properties.[1] As a membrane material, PVDF has been intensively studied for its application in ultrafiltration and microfiltration membrane,[2−4] protein adsorption, immobilization and separation,[5−7] waster water treatment,[8,9] proton conduction,[10−12] and stimuli-responsive controlled releases.[13−16] Graft copolymerization is a frequently adopted strategy in order to endow such specific functionalities to the existing PVDF homopolymers or commercial PVDF membranes. The radicals or radical-generating moieties are produced on the PVDF main chains or membrane surfaces initially, followed by the free-radical polymerization of the functional monomers alongside the PVDF main chains or on the membrane surface. The approaches to producing radicals or radical-generating moieties on the existing membranes have included irradiation by electron beam[9−12] and ion beam[17,18] and activation by plasma.[19−22] An alternative strategy involved the pretreatment of PVDF membrane in ethanolic KOH solution to form the unsaturated C═C bond on the membrane surface. Graft copolymer chains can also form on the PVDF membrane surface in the presence of benzyl peroxide and functional monomers.[23] On the other hand, peroxide initiators can be introduced onto the PVDF backbone by treatment of PVDF in solution with ozone. Subsequent graft copolymerization with a functional monomer gives rise to PVDF with functional side chains.[24]

As a controlled radical polymerization technique, atom transfer radical polymerization (ATRP) facilitates the control over the molecular weight, macromolecular architecture, and specific functionality.[25−27] More significantly, polymers prepared by ATRP have a living end functionality that can reinitiate further polymerization mediated by transition metals. ATRP has been employed to design and obtain PVDF-based block copolymers. For example, the poly(styrene)-*b*-poly(vinylidene fluoride)-*b*-poly(styrene) (PS-*b*-PVDF-*b*-PS) triblock copolymers were synthesized from the bromide-terminated PVDF macroinitiator (the *Br*-PVDF-*Br* telechelic polymer).[28] The poly(methyl methacrylate)-*b*-poly(vinylidene fluoride) (PMMA-*b*-PVDF) diblock copolymers and poly(methyl methacrylate)-*b*-poly(vinylidene fluoride)-*b*-poly(methyl methacrylate) (PMMA-*b*-PVDF-*b*-PMMA) triblock copolymers were synthesized from iodine-terminated monofunctional and bifunctional PVDF macroinitiators (PVDF-*I* and *I*-PVDF-*I* telechelic polymers, respectively).[29] To functionalize the PVDF membranes by controlled radical polymerization, vinylbenzyl chloride (VBC) was first graft copolymerized on the PVDF membrane surface via electron beam preirradiation. Subsequent ATRP of styrene was initiated from the benzyl chloride groups immobilized on the PVDF membrane surfaces.[30] The ATRP of poly(ethylene glycol) methacrylate initiated directly by the secondary $-CF_2-$ group of the PVDF main chains has also been reported.[31] Other reports indicate that the C−F bond cannot undergo homolytic cleavage to initiate ATRP of the monomers involved.[28−30,32−35]

The physical properties of the arborescent copolymers can differ to a great extent from those of their linear analogues. For example, water-soluble arborescent polystyrene (PS) copolymers had been constructed on the basis of the iterative grafting of end-functional polystyryllithium (PS-Li) chains onto reactive poly(chloroethyl vinyl) (PCEV) backbones, followed by chain extension of the external PS branches via living cationic polymerization of the protected hydrophilic vinyl ethers,

* To whom all correspondence should be addressed: Fax (65)-6779-1936; e-mail cheket@nus.edu.sg.

10.1021/ma048894l CCC: $27.50
Published on Web 08/17/2004

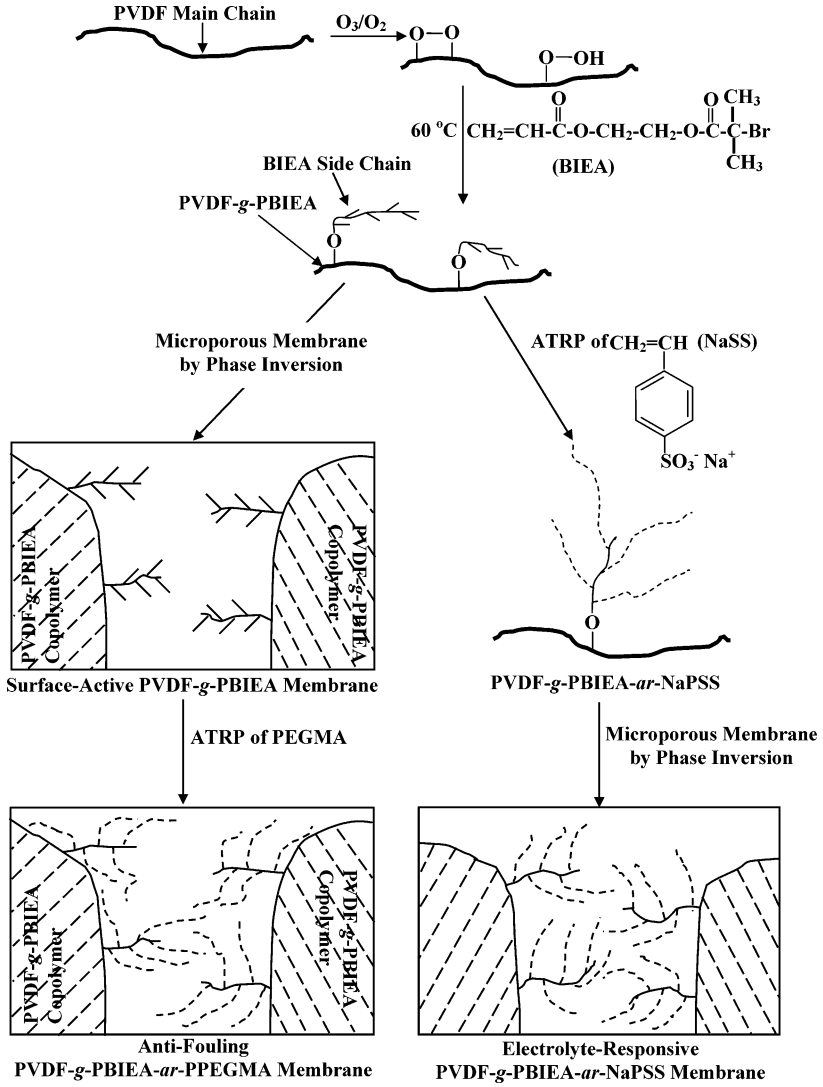

Figure 1. Schematic illustration of the process of ozone pretreatment and graft copolymerization of PVDF with inimer BIEA, preparation of "surface-active" PVDF-*g*-PBIEA membrane by phase inversion, the molecular functionalization of the PVDF-*g*-PBIEA graft copolymer via ATRP of NaSS, preparation of the electrolyte-responsive membrane from PVDF-*g*-PBIEA-*ar*-NaPSS copolymer by phase inversion, and surface-initiated ATRP of PEGMA on the PVDF-*g*-PBIEA membrane.

leading to polystyrene cores surrounded by a dense poly(vinyl ether) shell. Such arborescent copolymers can be made water-soluble and to behave like unimolecular nanoparticles in aqueous media by deprotection of the hydroxyl functions of the vinyl ether units.[36,37]

In this work, a novel PVDF graft copolymer with "living" side chains, from graft copolymerization of an ATRP inimer with the ozone-pretreated PVDF in solution, was prepared. ATRP of a functional monomer, initiated from the repeat units of the inimer side chains, gave rise to an arborescent copolymer. Both the initial PVDF−inimer graft copolymer and the arborescent copolymer could be cast into microporous membranes. The graft copolymer membrane with the active ATRP inimer repeat units on the surface could be further functionalized via surface-initiated ATRP. The reactions involved are illustrated schematically in Figure 1.

2. Experimental Section

2.1. Materials. Poly(vinylidene fluoride) (PVDF, Kynar K-761) powders (MW = 441 000) were obtained from Elf Atochem of North America Inc. They were used as received. 2-Hydroxyethyl acrylate (HEA) was obtained from Fluka Chemie of Neu-Ulm, Germany. The water content in HEA was removed by molecular sieve (20 nm). Triethylamine and 2-bromoisobutyl bromide were purchased from Aldrich Chemical Co. of Milwaukee, WI, and were used as received. Poly(ethylene glycol) methacryate (PEGMA) (MW = 360) was also obtained from Aldrich Chemical Co. The inhibitor in PEGMA was removed by column chromatography. The anionic monomer, sodium 4-styrenesulfonate (NaSS), the catalysts, copper(I) chloride (CuCl) and copper(II) chloride ($CuCl_2$), and the ligand for the ATRP, bipyridine (bPy), were also purchased from Aldrich Chemical Co. They were used as received. The solvents, *N*-methyl-2-pyrrolidone (NMP) and dimethyl sulfoxide (DMSO), were obtained from Merck Chemical Co. and Lab-Scan Asia Ltd. of Bangkok, Thailand, respectively. They were used as received.

2.2. Synthesis of the Inimer, 2-(2-Bromoisobutyryloxy)ethyl Acrylate (BIEA). The inimer, 2-(2-bromoisobutyryloxy)ethyl acrylate (BIEA), with the structure shown below, was synthesized according to the procedures reported in the literature.[38]

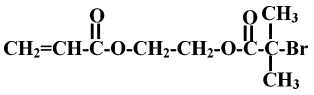

About 200 mL of dry THF, 20 mL of HEA (0.17 mol), and 25 mL of triethylamine (0.17 mol) were added into a 500 mL

flask, equipped with a magnetic follower and kept in an ice bath. 28 mL of 2-bromoisobutyl bromide (0.23 mol) was added into the flask dropwise through a funnel. After the addition, the flask was sealed, and the mixture was left to react at room temperature for 14 h. After the reaction, the mixture was washed with 3 × 200 mL of water to remove the THF, HEA residue, 2-bromoisobutylcarboxylic acid, and triethylammonium chloride. After drying over anhydrous $MgSO_4$, the remaining yellow liquid was distilled under vacuum at 75 °C for about 30 min. About 30 g of a yellow viscous liquid was obtained. Details on the polymerization of the inimer had been reported.[39,40]

2.2. Thermally Induced Graft Copolymerization of BIEA with the Ozone-Pretreated PVDF (PVDF-*g*-PBIEA Copolymer). The preparation of PVDF-*g*-PBIEA copolymer was carried out in a similar approach as reported earlier for the graft copolymerization of vinyl monomer with the ozone-pretreated PVDF.[41] The PVDF powders were dissolved in NMP to form a 7 wt % solution. A continuous O_3/O_2 mixture stream was bubbled through 30 mL of the PVDF/NMP solution at room temperature (~25 °C) for about 15 min, leading to a peroxide content of about 10^{-4} mol/g.[41] The O_3/O_2 mixture stream was generated from an Azcozon RMU16-40EM ozone generator. The flow rate was adjusted to 300 L/h to result in an ozone concentration of about 0.027 g/L in the gaseous mixture. After the ozone preactivation, the polymer solution was cooled in an ice bath. An argon stream was introduced for about 30 min to degas the ozone and oxygen dissolved in the solution.

Two grams of BIEA monomer and 12 mL of NMP were then added into the reaction mixture. After an additional 15 min of argon purging, the temperature of the water bath was raised to 60 °C to induce the decomposition of peroxide groups on the PVDF chains and to initiate the graft copolymerization of BIEA. After 6 h of reaction, the reaction mixture was cooled in an ice bath, and the resultant PVDF-*g*-PBIEA copolymer was precipitated in an excess amount of absolute ethanol. After filtering, the copolymer was redissolved in NMP and reprecipitated in ethanol. The copolymer was washed in an excess volume of ethanol for 48 h. The solvent was changed every 8 h. The copolymer sample was recovered and dried by pump under reduced pressure for subsequent characterization. The processes of ozone preactivation of PVDF and thermally induced graft copolymerization of BIEA are shown schematically in Figure 1.

2.3. Synthesis of the Arborescent Copolymer (PVDF-*g*-PBIEA-*ar*-NaPSS) via Atom Transfer Radical Polymerization (ATRP). 0.5 g of PVDF-*g*-PBIEA copolymer powder was introduced into 15 mL of DMSO. The temperature of the thermostated bath was increased to 50 °C to facilitate the dissolution, which took about 2 h. After the complete dissolution, the water bath was cooled to room temperature. An argon stream was introduced to degas the DMSO solution for 30 min. 2 g of sodium 4-styrenesulfonate (NaSS), 158 mg of 2,2′-bipyridine, 13.5 mg of $CuCl_2$, and 40 mg of CuCl were added to the solution. After the addition and dissolution, the solution became a brown liquid. The mixture was sealed and allowed to react at 40 °C for 6 h. At the end of the reaction, the reaction mixture was cooled in an ice bath, and the copolymer was precipitated in excessive ethanol. After recovery by filtration, the copolymer was washed in an excess volume of ethanol for 48 h. The solvent was changed every 8 h. The resulting arborescent copolymer (PVDF-*g*-PBIEA-*ar*-NaPSS) was recovered and dried by pump under reduced pressure for subsequent characterization. The preparation of the arborescent PVDF-*g*-PBIEA-*ar*-NaPSS copolymer is also shown schematically in Figure 1.

2.4. Fabrication of Microfiltration (MF) Membranes. The MF membranes of the PVDF-*g*-PBIEA and PVDF-*g*-PBIEA-*ar*-NaPSS copolymers were prepared by phase inversion. The copolymer powders were dissolved in NMP to a concentration of 12 wt % at room temperature. The copolymer solution was first cast onto a glass plate. The glass plate was subsequently immersed in doubly distilled water (and also in 1 M aqueous NaCl solution for the PVDF-*g*-PBIEA-*ar*-NaPSS copolymer). After the membrane had detached from the glass plates, it was extracted in a second bath of doubly distilled water at 70 °C for 15 min. This procedure was to stabilize the pore structure and to refine the pore size distribution. The purified MF membrane was dried by pump under reduced pressure for the subsequent characterization.

2.5. Surface-Initiated ATRP of PEGMA on PVDF-*g*-PBIEA MF membranes (PVDF-*g*-PBIEA-*ar*-PPEGMA Membrane). For the surface-initiated ATRP of the macromonomer, PEGMA, on the PVDF-*g*-PBIEA MF membrane, 15 mL of doubly distilled water, 2 mL of PEGMA, and 1 piece of the PVDF-*g*-PBIEA MF membrane of about 1 cm × 1 cm in area were added into a 25 mL single-necked round-bottom flask. A purified argon stream was introduced to degas the mixture for about 15 min. 158 mg of 2,2′-bipyridine, 13.5 mg of $CuCl_2$, and 40 mg of CuCl were added to the solution. The polymerization reaction was allowed to proceed for 1 h with stirring. After the reaction, the membrane was washed with copious amount of doubly distilled water over a period of about 2 h, followed by drying under reduced pressure. The process of the surface-initiated ATRP of PEGMA on the PVDF-*g*-PBIEA membrane is also shown schematically in Figure 1.

2.6. Fourier Transform Infrared (FTIR) and Nuclear Magnetic Resonance (NMR) Spectroscopies. After dispersion in KBr, the FTIR spectra of the copolymers were measured on a Bio-Rad FTS 135 FT-IR spectrophotometer. Each spectrum was collected by cumulating 16 scans at a resolution of eight wavenumbers. ^{1}H NMR spectroscopy of the PVDF-*g*-PBIEA copolymer was measured on a Bruker ARX 300 instrument at room temperature with deuterated DMSO as the solvent.

2.7. Thermogravimetric Analysis (TGA). The thermal stability of the copolymers was studied by thermogravimetric analysis (TGA). The samples were heated from room temperature to about 700 °C at a rate of 10 °C/min under a dry nitrogen atmosphere in a Du Pont Thermal Analyst 2100 system, equipped with a TGA 2050 thermogravimetric thermal analyzer.

2.8. X-ray Photoelectronic Spectroscopy (XPS). The surface composition of the membranes was measured by XPS. XPS measurements were carried out on a Kratos AXIS HSi spectrometer, under conditions similar to those reported in the earlier work.[41]

2.9. Scanning Electron Microscopy (SEM). The surface morphology of the MF membranes was studied by scanning electron microscopy (SEM), using a JEOL 6320 scanning electron microscope. The membranes were mounted on the sample studs by means of double-sided adhesive tapes. A thin layer of palladium was sputtered onto the membrane surface prior to the SEM measurement. The measurements were performed at an accelerating voltage of 15 kV.

2.10. Copolymer Composition Analysis. The carbon and bromide elemental contents were determined by the Microanalysis Laboratory, National University of Singapore. Taking into account the stoichiometries of the graft and the fluoropolymer chains, the bulk graft concentration of the PVDF-*g*-PBIEA copolymer, defined as the number of BIEA repeat units per repeat unit of PVDF, or the $([-\text{BIEA}-]/[-\text{CH}_2\text{CF}_2-])_{\text{bulk}}$ ratio, can be calculated from eq 1:

$$([-\text{BIEA}-]/[-\text{CH}_2\text{CF}_2-])_{\text{bulk}} = 2[\text{Br}]/([\text{C}] - 9[\text{Br}]) \quad (1)$$

where the factors 2 and 9 are introduced to account for the fact that there are 2 and 9 carbon atoms per repeat unit of PVDF and BIEA polymer, respectively. The graft concentration of NaSS in the PVDF-*g*-PBIEA-*ar*-NaPSS arborescent copolymer, or the $([-\text{NaSS}-]/[-\text{CH}_2\text{CF}_2-])_{\text{bulk}}$ ratio, is estimated from eq 2:

$$([-\text{NaSS}-]/[-\text{CH}_2\text{CF}_2-])_{\text{bulk}} = 2[\text{S}]/([\text{F}]) \quad (2)$$

where the factor 2 accounts for the fact that there are two

fluorine atoms per repeat unit of the PVDF polymer and one sulfur atom per repeat unit of the NaPSS polymer, respectively.

2.11. Protein Adsorption Assay. To assess the effect of surface-initiated ATRP of PEGMA from the PVDF-*g*-PBIEA membrane on the resistance of the latter to protein fouling, protein adsorption assays were performed on both the PVDF-*g*-PBIEA membrane and the PVDF-*g*-PBIEA-*ar*-PPEGMA membrane (time of polymerization = 1 h). The membranes (about 1 cm × 1 cm) were hydrated in methanol for 30 min initially, followed by washing three times with the phosphate-buffer saline (0.01 M PBS, pH = 7.4). The membranes were subsequently equilibrated in PBS solution for 1 h prior to the protein adsorption experiment. For the protein adsorption, the membranes were immersed in the PBS containing 2 mg/mL of γ-globulin for 24 h at room temperature. After the protein adsorption, the membranes were washed with copious amount of PBS and doubly distilled water. The membranes were dried by pumping under reduced pressure at room temperature. The surface composition of the membranes after protein adsorption was analyzed by XPS, using the N 1s signal as a marker for the adsorbed protein.

3. Results and Discussion

3.1. Preparation of the PVDF-*g*-PBIEA Graft Copolymer. 3.1.1. Preparation of the Inimer, 2-(2-Bromoisobutyryloxy)ethyl Acrylate (BIEA). The initiator monomer or the AB*-type "inimer" (A: polymerizable group; B*: initiator moiety) is designed for the synthesis of hyperbranched polymers because the AB* inimer can become involved in polymerization and initiation simultaneously.[42,43] For the addition polymerization, "A" typically represents the C=C double bond, while a variety of initiator moieties can be introduced as "B*". Examples of "B*" include an azo group for conventional radical polymerization,[44] an alkoxy or chloroalkyl group for living cationic polymerization,[42,45] an organolithium group for anionic living polymerization,[46] a nitroxide group for stable free radical polymerization,[47] an alkyl halide group for transition metal-catalyzed atom transfer radical polymerization (ATRP),[38−40] a dithioester group for photoinitiated addition−fragmentation chain transfer process,[48] and a trimethylsiloxyl group for group transfer polymerization (GTP).[49]

As a controlled radical polymerization technique, ATRP is versatile to a variety of monomers containing appropriate functional groups. In this study, the ATRP inimer, BIEA, was prepared via the esterification of HEA with 2-bromoisobutyryl bromide in dry THF and in the presence of triethylamine to neutralize the hydrogen bromide produced. The Fourier transform infrared (FTIR) spectra of HEA and BIEA were compared. After the esterification reaction, the absorption band at the wavenumber of about 3600 cm^{-1},[50] associated with the hydroxyl group of HEA, has disappeared almost completely, and the absorption band at the wavenumber of about 1740 cm^{-1}, associated with the ester carbonyl group,[50] has been enhanced. The results indicate that esterification reaction has occurred between HEA and 2-bromoisobutyryl bromide to form the AB* inimer, BIEA. The broad absorption band in the wavenumber region of 1100−1400 cm^{-1} is attributable to the dimethyl group of the initiator moiety.[50]

3.1.2. Ozone Pretreatment and Thermally Induced Graft Copolymerization of PVDF with BIEA: PVDF-*g*-PBIEA Copolymer. Ozone pretreatment of the PVDF solution was adopted to generate peroxide groups along the polymer main chain. The peroxide groups decomposed into radicals under thermal induction to initiate the chain polymerization of the vinyl monomer to produce the graft copolymer.[24,51] On the basis of the activation energy and Arrhenius coefficient reported in the literature, the half-life of this kind of peroxide groups is estimated to be about 45 min at 60 °C.[41] Thus, in this study, the time of polymerization was set at 6 h, both to increase the graft concentration of the BIEA side chains and to consume the peroxide residues completely.

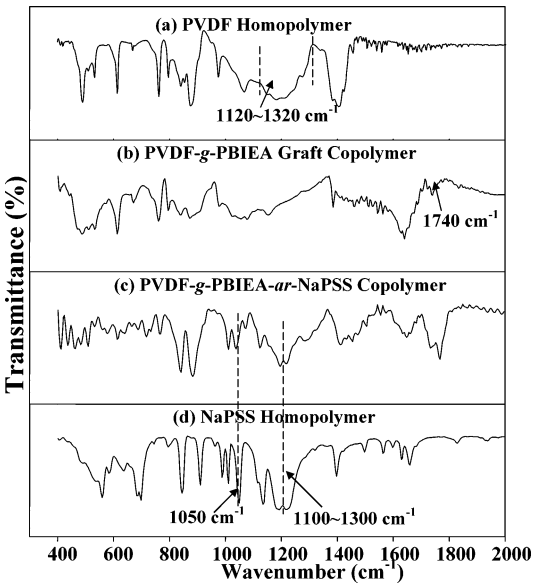

Figure 2. FTIR spectra of the (a) PVDF homopolymer, (b) PVDF-*g*-PBIEA copolymer, (c) PVDF-*g*-PBIEA-*ar*-NaPSS copolymer, and (d) NaPSS homopolymer.

Elemental analysis results indicate that the $([Br]/[C])_{bulk}$ ratio of the copolymer is about 0.02. The bulk graft concentration of the BIEA polymer (PBIEA) in PVDF-*g*-PBIEA, defined as the number of BIEA repeat units per repeat unit of PVDF, or the $([-BIEA-]/[-CH_2-CF_2-])_{bulk}$ ratio, is estimated by eq 1 (Experimental Section) to be about 0.05. Figure 2a,b shows the respective FTIR spectra of the pristine PVDF homopolymer and the PVDF-*g*-PBIEA copolymer. For the pristine PVDF homopolymer, the characteristic absorption band in the wavenumber region of 1120−1350 cm^{-1} is associated with the $-CF_2-$ group of the PVDF main chains.[50] A new absorption band at the wavenumber of about 1740 cm^{-1}, attributable to the ester carbonyl group,[50] has appeared after graft copolymerization with BIEA. Thus, the FTIR spectroscopic results confirm the presence of the BIEA side chains, in agreement with the results of the elemental analysis.

Figure 3 shows the thermal gravimetric analysis (TGA) curves of the PVDF homopolymer and the PVDF-*g*-PBIEA copolymer. The PVDF homopolymer exhibits only one thermal decomposition step, commencing at about 470 °C. On the other hand, the PVDF-*g*-PBIEA copolymer exhibited a two-step thermal decomposition process. The first main weight loss occurs at about 300 °C, attributable to degradation of the PBIEA side chains, while the second weight loss commences at about 470 °C, attributable to the decomposition of the PVDF main chains. The TGA curve also shows that the weight loss during the first decomposition step is about 14 wt %, which translates into a $([-BIEA-]/[-CH_2CF_2-])_{bulk}$ ratio of about 0.06. This ratio is comparable to that obtained from the elemental analysis. Both the FTIR

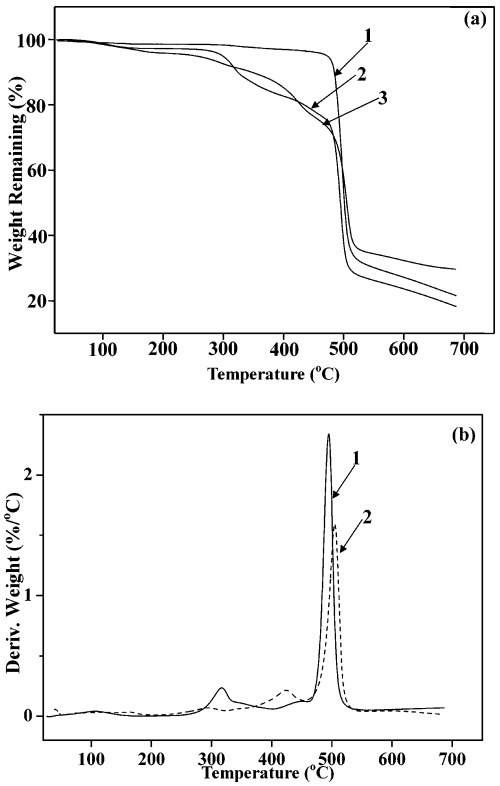

Figure 3. (a) TGA weight loss curves of (1) PVDF homopolymer, (2) PVDF-*g*-PBIEA copolymer ($[-BIEA-]/[-CH_2CF_2-]_{bulk} = 0.05$), and (3) PVDF-*g*-PBIEA-*ar*-NaPSS copolymer ($[-NaSS-]/[-CH_2CF_2-]_{bulk} = 0.22$). (b) TGA derivative curves of (1) the PVDF-*g*-PBIEA copolymer and (2) the PVDF-*g*-PBIEA-*ar*-NaPSS copolymer.

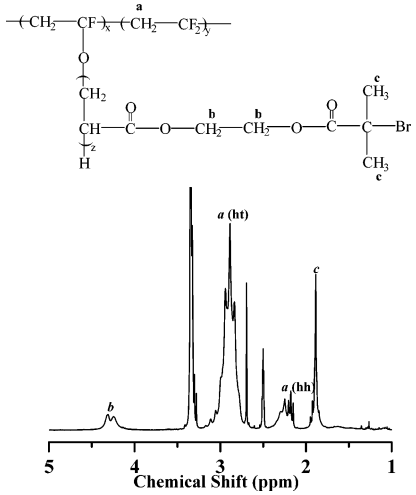

Figure 4. ^1H NMR spectrum of the PVDF-*g*-PBIEA copolymer.

spectra and the TGA results confirm that the BIEA have been graft-copolymerized with the ozone-pretreated PVDF main chains.

The chemical structure of the PVDF-*g*-PBIEA copolymer is shown in Figure 4 and verified by ^1H NMR spectroscopy. The chemical shifts at 2.9 and 2.2 ppm are attributable to the CH_2 species of PVDF, arising from the head-to-tail (ht) and head-to-head (hh) stereoregularities. On the other hand, the chemical shifts at 4.2−4.4 and 1.9−2.0 ppm are assigned to the $-CH_2CH_2-$ species and the isobutyryl species of the PBIEA side chains, respectively.[52] The ^1H NMR and the TGA results of the PVDF-*g*-PBIEA copolymer also indicate that transfer to the brominated monomer during graft copolymerization probably has not occurred to a significant extent, as the process can lead to cross-linking. The PVDF-*g*-PBIEA copolymer remains soluble and can be readily cast into porous membranes (see below).

3.2. PVDF-*g*-PBIEA Membranes Cast by Phase Inversion. The PVDF-*g*-PBIEA microporous membranes were fabricated by phase inversion in doubly distilled water at room temperature from 12 wt % NMP solutions of the PVDF-*g*-PBIEA copolymer. The morphology and surface chemical composition of the membrane were analyzed by SEM and XPS, respectively. Figure 5a,b shows the respective SEM images, obtained at a magnification of ×2000, for the air and glass substrate sides of the PVDF-*g*-PBIEA membranes. Thus, the PVDF-*g*-PBIEA copolymer can be cast into a microporous membrane by the phase inversion technique. Cross-sectional SEM images also indicate that the membrane is symmetric, although the porosity and pore size distribution for the two surfaces can differ substantially.

Figure 6a−c shows respectively the XPS wide-scan, Br 3d, and C 1s core-level spectra of the PVDF-*g*-PBIEA membrane. Carbon, bromine, fluorine, and oxygen signals are detected in the wide-scan spectrum of the PVDF-*g*-PBIEA membrane. The Br 3d core-level spectrum was resolved into Br $3d_{3/2}$ and Br $3d_{5/2}$ peak components with an energy separation of 1.05 eV. The Br $3d_{5/2}$ peak component with a binding energy at about 70.5 eV is characteristic of that of covalently bonded bromine.[53] The surface graft concentration of the PVDF-*g*-PBIEA membrane, or the $([-BIEA-]/[-CH_2CF_2-])_{surface}$ ratio, is determined to be about 0.07 from eq 1, based on the XPS-derived $([Br]/[C])_{surface}$ ratio of about 0.03. The $([-BIEA-]/[-CH_2CF_2-])_{surface}$ ratio is slightly higher than the bulk graft concentration of the PVDF-*g*-PBIEA copolymer, indicating that surface enrichment of the BIEA side chains occurs to some extent during the phase inversion process of the PVDF-*g*-PBIEA/NMP copolymer solution in water.

The C 1s core-level spectrum of the PVDF membrane was curve-fitted with peak components for the $-CH_2-$ and $-CF_2-$ species, at the BE of about 286.0 and 290.5 eV, respectively (Figure 6d).[54] The molar ratio of the two species, determined from the spectral area ratio of the two peak components, is about 1.06, in good agreement with the theoretical value of 1:1. The C 1s core-level spectrum of the PVDF-*g*-PBIEA membrane (Figure 6b) was curved-fitted with five species, adopting the following strategy. The peak components of approximately equal intensity with BE's at 286.0 and 290.5 eV are attributed to the $-CH_2-$ and $-CF_2-$ species, respectively, of the PVDF main chains. The peak components with BE's at about 284.6 and 288.8 eV are associated respectively with the neutral $-CH_2-$ and the O=C−O species of the BIEA side chains. The peak component with the BE at about 286.5 eV arises from combined contributions of the C−O species and the C−Br terminus of the BIEA side chains. For the comparison of the C 1s core-level spectra of the PVDF and PVDF-*g*-PBIEA membranes, it is clear that the peak intensity of the $-CF_2-$ species of the PVDF main chains has decreased substantially, after grafting of the BIEA side chains. The molar ratio of the $-CF_2-$ species to the total carbon species in the PVDF-*g*-PBIEA membrane is determined to be about 0.28, significantly lower than about 0.48 for the membrane prepared from the PVDF homopolymer.

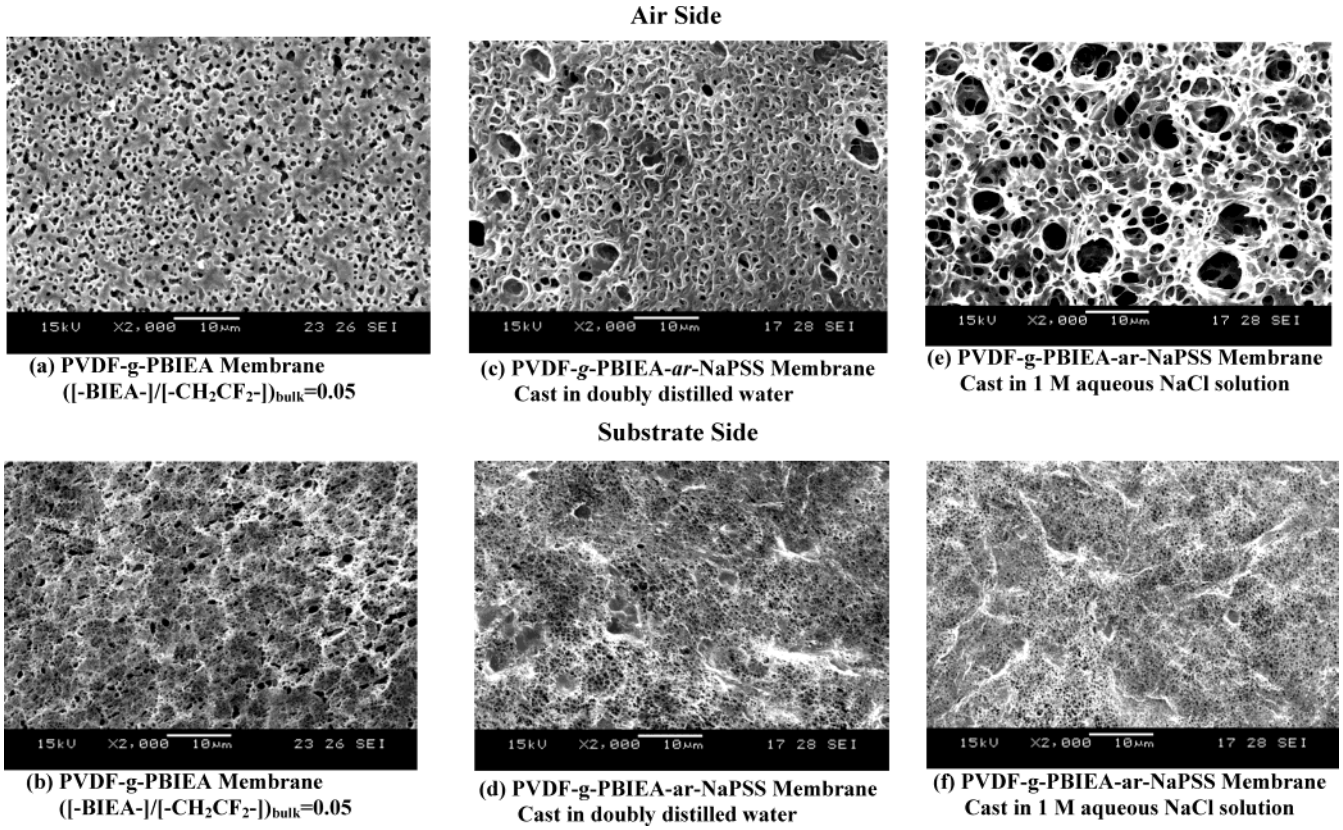

Figure 5. SEM micrographs of the membranes cast from the 12 wt % NMP solution of corresponding copolymer by phase inversion: (a) air side and (b) substrate (glass plate) side of PVDF-*g*-PBIEA membrane cast in water; (c) air and (d) substrate side of PVDF-*g*-PBIEA-*ar*-NaPSS membrane cast in water; (e) air and (f) substrate side of PVDF-*g*-PBIEA-*ar*-NaPSS membrane cast in 1 M aqueous NaCl solution.

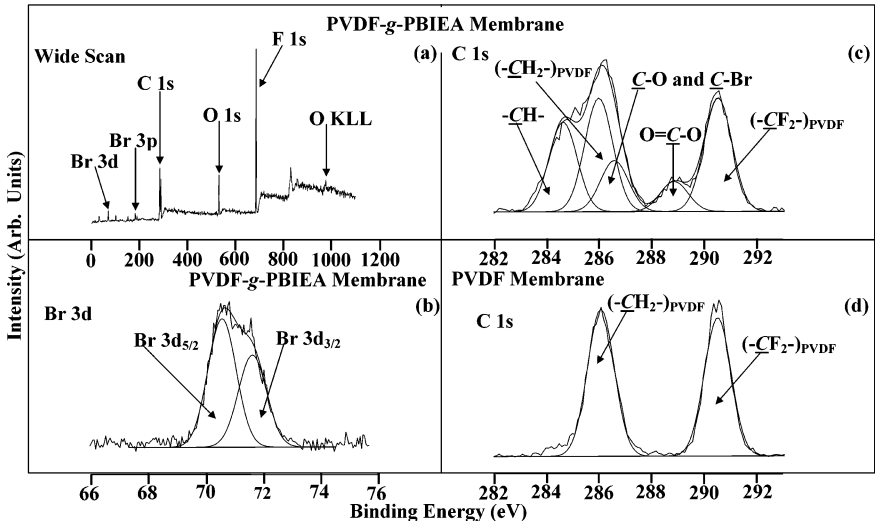

Figure 6. XPS wide-scan, Br 3d, and C 1s core-level spectra of the PVDF-*g*-PBIEA membrane and C 1s core-level spectrum of the PVDF membrane. Both membranes are cast from their corresponding 12 wt % NMP solution in doubly distilled water by the phase inversion technique.

3.3. The PVDF-*g*-PBIEA-*ar*-NaPSS Arborescent Copolymer via ATRP. The BIEA side chains of the PVDF-*g*-PBIEA copolymer and on the PVDF-*g*-PBIEA membrane surface can function as the ATRP macroinitiators because the tertiary C−Br moiety of each BIEA repeat unit will be able to initiate the ATRP of functional monomers.[25] The ATRP of substituted styrenic monomers had been well investigated using the Cu/bPy catalyst system.[55] In specific, the ATRP of sodium 4-styrenesulfonate (NaSS) has been carried out in the presence of the Cu(I)/bPy catalyst system in a water/methanol mixed medium to produce polyelectrolytes dissolved in solution or grafted on the silica particle surface.[56,57] As an amphiphilic polyelectrolyte, the NaSS polymer (NaPSS) can switch its conformation from an extended to a coiled state in an aqueous medium upon the addition of a low molecular weight electrolyte because the latter can shield the electrostatic repulsion among the sulfonate anions alongside the NaPSS chains. Thus, NaPSS exhibits an electrolyte-

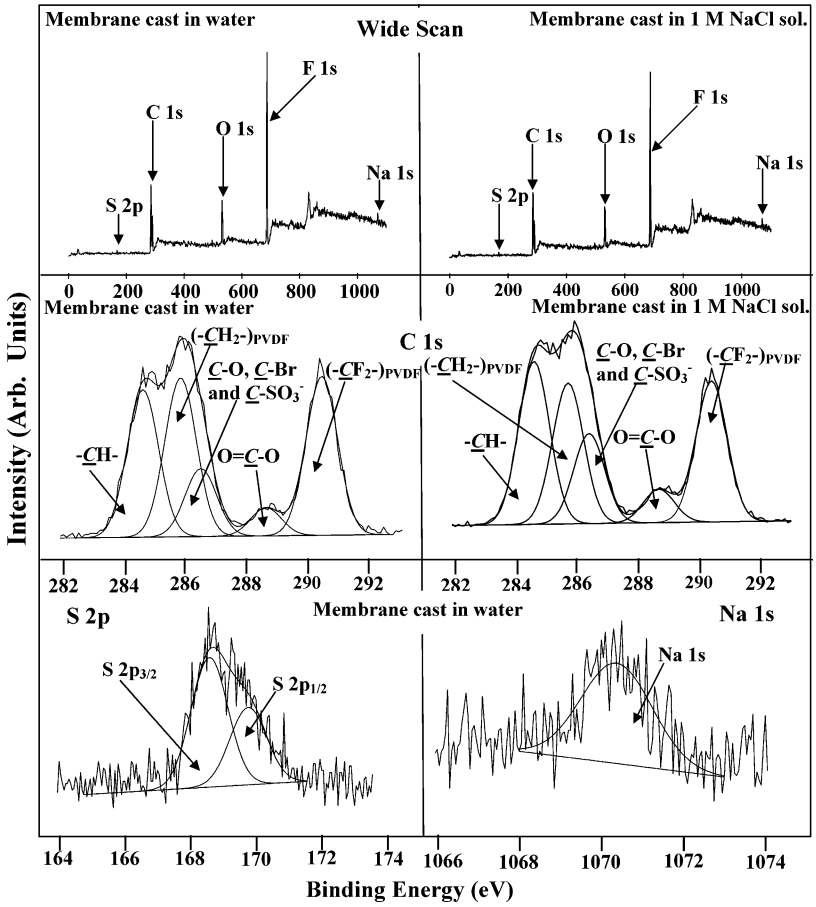

Figure 7. XPS wide-scan, C 1s, S 2p, and Na 1s core-level spectra of the PVDF-*g*-PBIEA-*ar*-NaPSS membranes cast from the 12 wt % NMP solution by phase inversion in doubly distilled water and in 1 M aqueous NaCl solution.

responsive behavior (the polyelectrolyte effect).[58−60]

The arborescent copolymer with the NaPSS side chains, or the PVDF-*g*-PBIEA-*ar*-NaPSS copolymer, was prepared via solution polymerization of NaSS, initiated by the BIEA repeat units of the PVDF-*g*-PBIEA copolymer and catalyzed by the $CuCl/CuCl_2$/bPy system in DMSO. The sulfur, fluorine, and carbon contents of the PVDF-*g*-PBIEA-*ar*-NaPSS copolymer were determined by elemental analysis. The $([S]/[F])_{bulk}$ ratio of the copolymer was determined to be about 0.11. Thus, the bulk graft concentration, defined as the number of NaSS repeat units per PVDF repeat unit, or the $([-NaSS-]/[-CH_2CF_2-])_{bulk}$ ratio, is determine to be about 0.22 (eq 2, Experimental Section). The FTIR spectra of the PVDF-*g*-PBIEA-*ar*-NaPSS copolymer and NaPSS homopolymer are shown and compared in Figure 2. After copolymerization with NaSS, a new absorption band in the wavenumber region of 1050 cm^{-1}, associated with the sulfonate groups of the NaPSS side chains,[50] appears in the FTIR spectrum of the PVDF-*g*-PBIEA-*ar*-NaPSS copolymer. On the other hand, the absorption band in the wavenumber region of 1100−1300 cm^{-1}, corresponding to the aromatic C−H in-plane bending mode,[50] also serves to indicate that the NaPSS side chains have been incorporated into the copolymer.

The TGA curve of the PVDF-*g*-PBIEA-*ar*-NaPSS copolymer was compared to that of PVDF-*g*-PBIEA polymer in Figure 3. Figure 3a shows the weight loss curves of the PVDF homopolymer, the PVDF-*g*-PBIEA copolymer, and the PVDF-*g*-PBIEA-*ar*-NaPSS copolymer. In comparison with the PVDF-*g*-PBIEA copolymer, the PVDF-*g*-PBIEA-*ar*-NaPSS copolymer exhibits a large weight loss in the temperature range of 300−480 °C, attributable to the decomposition of the PBIEA and NaPSS graft chains. Figure 3b shows the derivative of the weight curves as a function of the temperature for the PVDF-*g*-PBIEA and PVDF-*g*-PBIEA-*ar*-NaPSS copolymers. For the PVDF-*g*-PBIEA copolymer, the derivative curve contains two major peaks at temperatures of 310 and 490 °C, attributable to the PBIEA side chains and PVDF main chains, respectively. However, for the PVDF-*g*-PBIEA-*ar*-NaPSS copolymer, these two peaks diminish, and a new decomposition peak emerges at the temperature of about 425 °C, attributable to the NaPSS side chains. The NaPSS content of the copolymer cannot be determined unambiguously from the weight loss curve of the copolymer. Attempts were made to improve the bulk graft concentration of NaPSS in the PVDF-*g*-PBIEA-*ar*-NaPSS copolymer by increasing the NaSS monomer concentration in the reaction mixture or extending the time of polymerization from 6 to 12 h. It was found that the solubility of the PVDF-*g*-PBIEA-*ar*-NaPSS copolymer in NMP was compromised by the high content of NaPSS. Therefore, the ATRP of NaSS initiated from PVDF-*g*-PBIEA was not carried out at a higher monomer feed ratio or for a longer polymerization time.

3.4. Electrolyte-Responsive Membrane Cast from the PVDF-*g*-PBIEA-*ar*-NaPSS Copolymer. The morphology, surface composition, and the electrolyte-responsive nature of the PVDF-*g*-PBIEA-*ar*-NaPSS membranes were investigated. Figure 7 shows the respective XPS wide-scan, C 1s, S 2p, and Na 1s core-level spectra of the PVDF-*g*-PBIEA-*ar*-NaPSS mem-

branes cast from a 12 wt % NMP solution of the PVDF-*g*-PBIEA-*ar*-NaPSS copolymer by phase inversion in doubly distilled water and in 1 M aqueous NaCl solution. In the wide-scan spectra of the two membranes, not only are the C 1s, F 1s, and O 1s signals detected, the Na 1s and S 2p signals are also discernible. For both membranes, the intensity of the Br 3d signal for the PVDF-*g*-PBIEA-*ar*-NaPSS membrane has been reduced considerably, in comparison with that of the Br 3d signal for the PVDF-*g*-PBIEA membrane. The membrane cast in 1 M aqueous NaCl solution exhibits higher Na 1s and S 2p signal intensities compared to those of the membrane cast in water. The XPS-derived surface elemental composition, or the $([C]:[Na]:[S]:[Br])_{surface}$ ratio, determined from the respective spectral peak areas, shifted from 100:1.3:2.0:0.3 to 100:4.0:4.6:0.8 when the ionic strength of the casting bath was increased from about 0 (for doubly distilled water) to 1 M (for the 1 M aqueous NaCl solution). Thus, the surface composition data indicate a significant surface enrichment of the PBIEA-*g*-NaPSS side chains for the membrane cast in 1 M aqueous NaCl solution.

The C 1s core-level spectra of the PVDF-*g*-PBIEA-*ar*-NaPSS membranes cast in doubly distilled water and in 1 M aqueous NaCl solution were curve-fitted using the approach similar to that used for the PVDF-*g*-PBIEA membrane, except that the peak component with BE at about 286.5 eV is deemed to have resulted from a combined contribution from the *C*−O, *C*−Br, and *C*−SO_3 species.[61] From the C 1s spectra, it is clear that the intensity of the −*C*H− species, associated with the PBIEA-*g*-NaPSS side chain, increases while that of the $(-CF_2-)_{PVDF}$ species decreases when the ionic strength of the casting bath is increased to 1 M. The XPS-derived $([-CF_2-]_{PVDF}/[-CH-])_{surface}$ ratio, determined from the corresponding C 1s peak component spectral area ratio, decreases from 1.1 to 0.86, suggesting that more PBIEA-*g*-NaPSS side chains have migrated from the bulk to the surface during the phase inversion process in 1 M aqueous NaCl solution. The S 2p core-level spectrum of the PVDF-*g*-PBIEA-*ar*-NaPSS membrane, cast in doubly distilled water, was curve-fitted with S $2p_{1/2}$ and S $2p_{3/2}$ peak components with an energy separation of 1.2 eV, as shown in Figure 7.

The microporous morphology of the PVDF-*g*-PBIEA-*ar*-NaPSS membranes is also dependent on the electrolyte concentration. Figure 5c−f shows the respective SEM micrographs, obtained at a magnification of ×2000, for the air side and substrate side of the PVDF-*g*-PBIEA-*ar*-NaPSS membranes cast in doubly distilled water and in 1 M aqueous NaCl solution. With the increase in ionic strength of the casting bath, the morphology and pore structure do not change significantly on the substrate side. However, significant differences in the surface morphology and pore structure are observed on the air side of the PVDF-*g*-PBIEA-*ar*-NaPSS membrane. The membrane cast in 1 M aqueous NaCl solution exhibits a much larger pore size and a less uniform pore size distribution, in comparison to those of the membrane cast in doubly distilled water. When cast in the aqueous NaCl medium, the membrane surfaces is enriched by the NaPSS chains. Pores of larger size are formed to minimize the interfacial interaction between the membrane surface and the aqueous electrolyte medium, as larger pores correspond to smaller specific surface area. The cross-sectional SEM images of the PVDF-*g*-PBIEA-*ar*-NaPSS membranes revealed a "through pore" structure of the membrane, although the pore size differs on both sides of the membrane.

The nature of the NaPSS side chain as a polyelectrolyte accounts for the electrolyte-responsive characteristics of the surface chemical composition and morphology of the PVDF-*g*-PBIEA-*ar*-NaPSS copolymer membrane. When the PVDF-*g*-PBIEA-*ar*-NaPSS polymer solution was cast into doubly distilled water, the strong electrostatic repulsion among the sulfonate anions alongside the NaPSS chains on the newly formed membrane surface prohibited extensive migration of the NaSS side chains from the bulk of the polymer solution to the outer layer of the membranes. On the other hand, when cast into 1 M aqueous NaCl solution, the electrostatic repulsion was mostly shielded by the electrolyte ions in the casting bath (polyelectrolyte effect), allowing more extensive migration of the NaPSS side chains to the membrane surface, including the surface of the pores.

3.5. Functionalization of the PVDF-*g*-PBIEA Membrane via Surface-Initiated ATRP of the Poly(ethylene glycol) Methacrylate (PEGMA): Antifouling PVDF-*g*-PBIEA-*ar*-PPEGMA Membrane. For the porous membrane cast from the PVDF-*g*-PBIEA copolymer, each repeat unit of the PBIEA side chains on the membrane and pore surfaces can initiate the ATRP of a functional monomer to endow specific surface functionalities to the as-cast PVDF-*g*-PBIEA membranes. Poly(ethyl glycol) (PEG) and poly(ethylene oxide) (PEO) have attracted considerable attention because they can impart antifouling, nonadhesive, and biocompatible characteristics to the materials.[62,63] ATRP of the PEGMA macromonomer has been extensively studied during the past few years because the process allows the preparation of well-defined PEGMA polymer (PPEGMA).[64−66] The Cu/bPy catalyst system can also result in a controlled fashion in the ATRP of methacrylate monomer;[66,67] therefore, in this study, PEGMA was graft copolymerized directly onto the PVDF-*g*-PBIEA membrane surface, via ATRP in an aqueous medium and catalyzed by the $CuCl/CuCl_2$/bPy system, with the intention of improving the antifouling properties of the PVDF-*g*-PBIEA membrane.

Figure 8a shows the XPS wide-scan and C 1s core-level spectra of the PVDF-*g*-PBIEA-*ar*-PPEGMA membrane after 1 h of surface-initiated ATRP of PEGMA. Compared to those of the PVDF-*g*-PBIEA membrane (see Figure 6), significant changes in the XPS wide-scan and C 1s core-level spectra of the PVDF-*g*-PBIEA-*ar*-PPEGMA membrane are observed. The F 1s signals associated with the underlying PVDF main chains are no longer discernible in the wide-scan spectrum, indicating that the thickness of the PEGMA polymer film on the PVDF-*g*-PBIEA membrane surface, after a 1 h of polymerization, has exceeded the sampling depth of the XPS technique (∼7.5 nm for organic matrix[68]). The same result is also deduced from the changes in the C 1s core-level line shape of the PVDF-*g*-PBIEA-*ar*-PPEGMA membrane. The C 1s core-level spectrum of the PVDF-*g*-PBIEA-*ar*-PPEGMA membrane was curve-fitted using the similar approach as that for the PVDF-*g*-PBIEA membrane. However, the two species associated with the PVDF main chains, $(-CH_2-)_{PVDF}$ and $(-CF_2-)_{PVDF}$ with BE's at 285.8 and 290.5 eV, respectively, have disappeared completely. On the other hand, the peak component with a BE of about 286.2 eV,

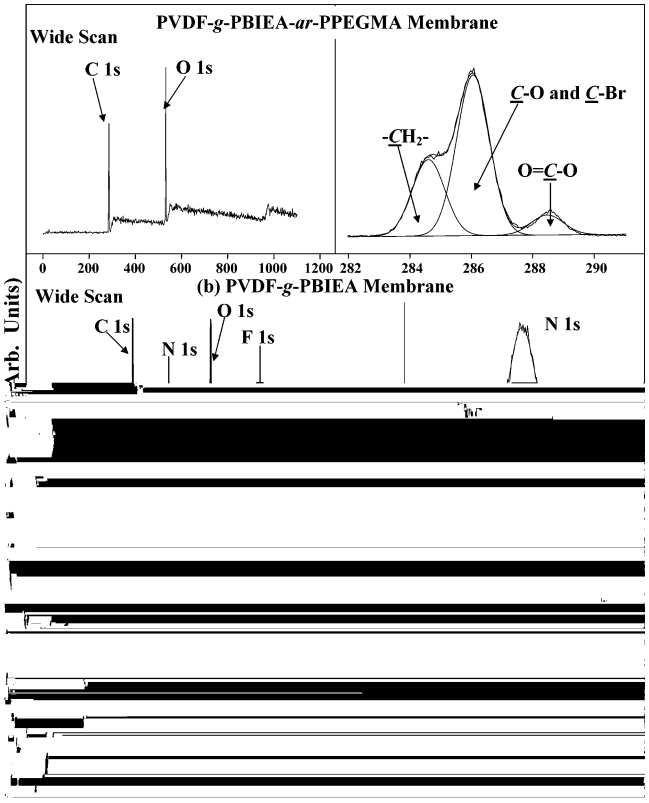

Figure 8. (a) XPS wide-scan and C 1s core-level spectra of the PVDF-*g*-PBIEA-*ar*-PPEGMA membrane (time of polymerization = 1 h); XPS wide-scan and N 1s core-level spectra of (b) the PVDF-*g*-PBIEA membrane and (c) PVDF-*g*-PBIEA-*ar*-PPEGMA membrane after a 24 h of γ-globulin adsorption.

attributed to the *C*−O species of the PBIEA and PPEGMA side chains, has been greatly enhanced. Similar to that of the PVDF-*g*-PBIEA-*ar*-NaPSS membrane cast from the PVDF-*g*-PBIEA-*ar*-NaPSS copolymer, the intensity of the Br 3d component has been greatly reduced after the surface-initiated ATRP of PEGMA with the PVDF-*g*-PBIEA membrane. The $([Br]/[C])_{surface}$ ratio has decreased from 0.03 to about 0.02, arising probably from the irreversible termination and halogen exchange of the propagating radicals during the surface-initiated ATRP process.[69−71]

Protein adsorption study on both the PVDF-*g*-PBIEA membrane and the PVDF-*g*-PBIEA-*ar*-PPEGMA membrane was carried out to evaluate the antifouling properties of the membrane surface after the surface-initiated ATRP of PEGMA. The amount of surface-adsorbed protein (γ-globulin) was quantified by XPS because the N 1s signal associated with γ-globulin can be used as a convenient marker for the protein. Figure 8b,c shows the respective XPS wide-scan and N 1s core-level spectra of the PVDF-*g*-PBIEA and PVDF-*g*-PBIEA-*ar*-PPEGMA membranes after 24 h of exposure to 2 mg/mL γ-globulin solution. For the PVDF-*g*-PBIEA membrane, in addition to the Br 3d, C 1s, O 1s, and F 1s signals of the PVDF-*g*-PBIEA membrane substrates, a strong N 1s signal at the BE of about 399.3 eV was also detected in the wide-scan spectrum. After the surface-initiated ATRP of PEGMA on the PVDF-*g*-PBIEA membrane, the membrane exhibited significant resistance to protein adsorption. For the PVDF-*g*-PBIEA-*ar*-PPEGMA membrane, the wide-scan spectrum is dominated by the C 1s and O 1s signals while the N 1s signal is barely discernible. The N 1s core-level spectra of the two membranes are also compared in Figure 8. The $([N]/[C])_{surface}$ ratios, determined from the respective peak component area ratios, were about 0.02 and 0.16 for the PVDF-*g*-PBIEA-*g*-PPEGMA membrane and PVDF-*g*-PBIEA membrane, respectively. These results indicate that the antifouling property of the PVDF-*g*-PBIEA membrane has been improved substantially by the surface-initiated ATRP of PEGMA.

4. Conclusions

PVDF with grafted ATRP inimer, BIEA, side chains allowed the preparation of arborescent copolymer. Both the PVDF-*g*-PBIEA and its arborescent copolymer of a polyelectrolyte, NaPSS, could be readily cast into microporous membranes with surface-enriched graft chains via phase inversion in an aqueous medium. The surface composition and morphology of the PVDF-*g*-PBIEA-*ar*-NaPSS membranes exhibited electrolyte-responsive behavior. The BIEA units on the PVDF-*g*-PBIEA membranes could serve as the macroinitiators for the surface-initiated ATRP to further functionalize the membrane. The inimer graft copolymerization technique provided an alternative approach to the functionalization of membranes both at the molecular level (prior to the casting of membrane) and at the membrane surface level. Because of the end functionality associated with the ATRP technique, such membrane surface exhibited a "living" character, allowing for additional surface-initiated reactions to introduce well-defined functional polymers and moieties. The porous membrane with active or "living" surfaces thus provides exciting opportunities for the direct molecular design and engineering of the membrane and pore surfaces.

References and Notes

(1) Jungnickel, B. J. In *The Polymeric Materials Encyclopedia*; Salamone, J. C., Ed.; CRC Press: Boca Raton, FL, 1996; Vol. 7, pp 7115−7123.
(2) Bessieres, A.; Meireles, M.; Coratger, R.; Beauvillain, J.; Sanchez, V. *J. Membr. Sci.* **1996**, *109*, 271.
(3) Yeow, M. L.; Liu, Y. T.; Li, K. *J. Appl. Polym. Sci.* **2004**, *92*, 1782.
(4) Li, K. *Chem. Eng. Technol.* **2002**, *25*, 203.
(5) Vestling, M. M.; Fenselau, C. *Mass Spectrom. Rev.* **1995**, *14*, 169.
(6) Mueller, J.; Davis, R. H. *J. Membr. Sci.* **1996**, *116*, 47.
(7) Sutton, C. W.; Wheeler, C. H.; Sally, U.; Corbett, J. M.; Dunn, M. J. *Electrophoresis* **1997**, *18*, 424.
(8) Jian, K.; Pintauro, P. N.; Ponangi, R. *J. Membr. Sci.* **1996**, *117*, 117.
(9) Banat, F. A.; Simandl, J. *J. Membr. Sci.* **1999**, *163*, 333.
(10) Hietala, S.; Holmberg, S.; Karjalainen, M.; Nasman, J.; Paronen, M.; Serimaa, R.; Sundholm, F.; Vahvaselka, S. *J. Mater. Chem.* **1997**, *7*, 721.
(11) Mattsson, B.; Ericson, H.; Torell, L. M.; Sundholm, F. *J. Polym. Sci., Part A: Polym. Chem.* **1999**, *37*, 3317.
(12) Hietala, S.; Maunu, S. L.; Sundholm, F.; Lehtinen, T.; Sundholm, G. *J. Polym. Sci., Part B: Polym. Phys.* **1999**, *37*, 2893.
(13) Akerman, S.; Viinikka, P.; Svarfvar, B.; Jarvinen, K.; Kontturi, K.; Nasman, J.; Urtti, A.; Paronen, P. *J. Controlled Release* **1998**, *50*, 153.
(14) Akerman, S.; Viinikka, P.; Svarfvar, B.; Putkonen, K.; Jarvinen, K.; Kontturi, K.; Nasman, J.; Urtti, A.; Paronen, P. *Int. J. Pharm.* **1998**, *164*, 29.
(15) Akerman, S.; Svarfvar, B.; Kontturi, K.; Nasman, J.; Urtti, A.; Paronen, P.; Jarvinen, K. *Int. J. Pharm.* **1999**, *178*, 67.
(16) Tarvainen, T.; Svarfvar, B.; Akerman, S.; Savolainen, J.; Karhu, M.; Paronen, P.; Jarvinen, K. *Biomaterials* **1999**, *20*, 2177.
(17) Daubresse, C.; SergentEngelen, T.; Ferain, E.; Schneider, Y. J.; Legras, R. *Nucl. Instrum. Methods B* **1995**, *105*, 126.
(18) Betz, N.; Begue, J.; Goncalves, M.; Gionnet, K.; Deleris, G.; Le Moel, A. *Nucl. Instrum. Methods B* **2003**, *208*, 434.

(19) Lee, Y. M.; Shim, I. K. *J. Appl. Polym. Sci.* **1996**, *61*, 1245.
(20) Chang, C. L.; Chang, M. S. *Desalination* **2002**, *148*, 39.
(21) Klee, D.; Ademovic, Z.; Bosserhoff, A.; Hoecker, H.; Maziolis, G.; Erli, H. J. *Biomaterials* **2003**, *24*, 3663.
(22) Hsueh, C. L.; Peng, Y. J.; Wang, C. C.; Chen, C. Y. *J. Membr. Sci.* **2003**, *219*, 1.
(23) Qiu, X. P.; Li, W. Q.; Zhang, S. C.; Liang, H. Y.; Zhu, W. T. *J. Electrochem. Soc.* **2003**, *150*, A917.
(24) Boutevin, B.; Robin, J. J.; Serdani, A. *Eur. Polym. J.* **1992**, *28*, 1507.
(25) Matyjaszewski, K.; Xia, J. H. *Chem. Rev.* **2001**, *101*, 2921.
(26) Kamigaito, M.; Ando, T.; Sawamoto, M. *Chem. Rev.* **2001**, *101*, 3689.
(27) Coessens, V.; Pintauer, T.; Matyjaszewski, K. *Prog. Polym. Sci.* **2001**, *26*, 337.
(28) Zhang, Z. B.; Ying, S. K.; Shi, Z. Q. *Polymer* **1999**, *40*, 1341.
(29) Jo, S. M.; Lee, W. S.; Ahn, B. S.; Park, K. Y.; Kim, K. A.; Paeng, I. S. R. *Polym. Bull. (Berlin)* **2000**, *44*, 1.
(30) Holmberg, S.; Holmlund, P.; Wilen, C. E.; Kallio, T.; Sundholm, G.; Sundholm, F. *J. Polym. Sci., Part A: Polym. Chem.* **2002**, *40*, 591.
(31) Hester, J. F.; Banerjee, P.; Won, Y. Y.; Akthakul, A.; Acar, M. H.; Mayes, A. M. *Macromolecules* **2002**, *35*, 7652.
(32) Zhang, Z. B.; Ying, S. K.; Shi, Z. Q. *Polymer* **1999**, *40*, 5439.
(33) Destarac, M.; Matyjaszewski, K.; Silverman, E.; Ameduri, B.; Boutevin, B. *Macromolecules* **2000**, *33*, 4613.
(34) Becker, M. L.; Remsen, E. E.; Wooley, K. L. *J. Polym. Sci., Part A: Polym. Chem.* **2001**, *39*, 4152.
(35) Li, K.; Wu, P. P.; Han, Z. W. *Polymer* **2002**, *43*, 4079.
(36) Muchtar, Z.; Schappacher, M.; Deffieux, A. *Macromolecules* **2001**, *34*, 7595.
(37) Schappacher, M.; Deffieux, A.; Putaux, J. L.; Viville, P.; Lazzaroni, R. *Macromolecules* **2003**, *36*, 5776.
(38) Matyjaszewski, K.; Gaynor, S. G.; Kulfan, A.; Podwika, M. *Macromolecules* **1997**, *30*, 5192.
(39) Matyjaszewski, K.; Pyun, J.; Gaynor, S. G. *Macromol. Rapid Commun.* **1998**, *19*, 665.
(40) Matyjaszewski, K.; Gaynor, S. G. *Macromolecules* **1997**, *30*, 7042.
(41) Wang, P.; Tan, K. L.; Kang, E. T.; Neoh, K. G. *J. Mater. Chem.* **2001**, *11*, 783.
(42) Frechet, J. M. J.; Henmi, M.; Gitsov, I.; Aoshima, S.; Leduc, M. R.; Grubbs, R. B. *Science* **1995**, *269*, 1080.
(43) Mori, H.; Muller, A. H. E. *Top. Curr. Chem.* **2003**, *228*, 1.
(44) Kricheldorf, H. R.; Zang, Q. Z.; Schwarz, G. *Polymer* **1982**, *23*, 1821.
(45) Paulo, C.; Puskas, J. E. *Macromolecules* **2001**, *34*, 734.
(46) Baskaran, D. *Polymer* **2003**, *44*, 2213.
(47) Hawker, C. J.; Frechet, J. M. J.; Grubbs, R. B.; Dao, J. *J. Am. Chem. Soc.* **1995**, *117*, 10763.
(48) Ishizu, K.; Ohta, Y.; Kawauchi, S. *Macromolecules* **2002**, *35*, 3781.
(49) Simon, P. F. W.; Muller, A. H. E. *Macromolecules* **2001**, *34*, 6206.
(50) *The Systematic Identification of Organic Compounds*, 7th ed.; Shriner, R. L., Hermann, C. K. E., Morrill, T. C., Curtin, D. Y., Fuson, R. C., Eds.; J. Wiley & Sons: New York, 1998.
(51) Karlsson, J. O.; Gatenholm, P. *Macromolecules* **1999**, *32*, 7594.
(52) Mori, H.; Walther, A.; Andre, X.; Lanzendorfer, M. G.; Muller, A. H. E. *Macromolecules* **2004**, *37*, 2054.
(53) Touihri, S.; Bernede, J. C.; Molinie, P.; Legoff, D. *Polymer* **2002**, *43*, 3123.
(54) *The Handbook of X-ray Photoelectron Spectroscopy*, 2nd ed.; Moulder, J. F., Stickle, W. F., Sobol, P. E., Bomben, K., Eds.; Perkin-Elmer Corporation (Physical Electronics): Wellesley, MA, 1992; pp 216−217.
(55) Qiu, J.; Matyjaszewski, K. *Macromolecules* **1997**, *30*, 5643.
(56) Iddon, P. D.; Robinson, K. L.; Armes, S. P. *Polymer* **2004**, *45*, 759.
(57) Chen, X. Y.; Randall, D. P.; Perruchot, C.; Watts, J. F.; Patten, T. E.; von Werne, T.; Armes, S. P. *J. Colloid Interface Sci.* **2003**, *257*, 56.
(58) Lowe, A. B.; McCormick, C. L. In *Stimuli-Responsive Water Soluble and Amphiphilic Polymers*, 2nd ed.; McCormick, C. L., Ed.; American Chemical Society: Washington, DC, 2000; Vol. 780, pp 1−13.
(59) McCormick, C. L.; Kathmann, E. E. In *The Polymeric Materials Encyclopedia*; Salamone, J. C., Ed.; CRC Press: Boca Raton, FL, 1996; Vol. 7, pp 7189−7201.
(60) Valencia, J.; Pierola, I. F. *Eur. Polym. J.* **2001**, *37*, 2345.
(61) Ruangchuay, L.; Schwank, J.; Sirivat, A. *Appl. Surf. Sci.* **2002**, *199*, 128.
(62) Feldman, K.; Hahner, G.; Spencer, N. D.; Harder, P.; Grunze, M. *J. Am. Chem. Soc.* **1999**, *121*, 10134.
(63) Dalsin, J. L.; Hu, B. H.; Lee, B. P.; Messersmith, P. B. *J. Am. Chem. Soc.* **2003**, *125*, 4253.
(64) Ali, M. M.; Stover, H. D. H. *Macromolecules* **2003**, *36*, 1793.
(65) Robinson, K. L.; de Paz-Banez, M. V.; Wang, X. S.; Armes, S. P. *Macromolecules* **2001**, *34*, 5799.
(66) Neugebauer, D.; Zhang, Y.; Pakula, T.; Sheiko, S. S.; Matyjaszewski, K. *Macromolecules* **2003**, *36*, 6746.
(67) Wang, J. L.; Grimaud, T.; Matyjaszewski, K. *Macromolecules* **1997**, *30*, 6507.
(68) Tan, K. L.; Woon, L. L.; Wong, H. K.; Kang, E. T.; Neoh, K. G. *Macromolecules* **1993**, *26*, 2832.
(69) Davis, K. A.; Matyjaszewski, K. *Macromolecules* **2001**, *34*, 2101.
(70) Matyjaszewski, K.; Wang, J. L.; Grimaud, T.; Shipp, D. A. *Macromolecules* **1998**, *31*, 1527.
(71) Matyjaszewski, K.; Shipp, D. A.; Wang, J. L.; Grimaud, T.; Patten, T. E. *Macromolecules* **1998**, *31*, 6836.

MA048894L